Fault Diagnosis of Fire Hydraulic System based on 1DCNN-Bayesian Optimization

Wenhong Fu, Zhihua Hu*

School of Intelligent Manufacturing and Control Engineering, Shanghai Polytechnic University, Shanghai, 201209, China

Abstract

To solve the problem of low efficiency and scarce fault data caused by the traditional fault diagnosis of fire hydraulic system relying on manual experience, this paper proposes an intelligent diagnosis method integrating simulation modeling and 1DCNN-Bayesian optimization. Methods: Firstly, a fire hydraulic system model was built based on Simscape, and the effectiveness of the model was verified by comparing the performance curve of the fire pump. Secondly, a 1DCNN model was constructed, and the Bayesian optimization algorithm was introduced to automatically search for the optimal network structure. Results: The root mean square error of the head-flow performance curve of the fire pump was 0.13m, and the root mean square error of the effective shaft power-flow performance curve was 13.05w, indicating the data effectiveness of the simulation model; the accuracy of the 1DCNN model after Bayesian optimization reached 98.51%, which was 1.50% higher than the original model. The optimal configuration was: three-layer convolution (kernel size [20,5,3], number of filters [32,64,128]), Dropout parameter was 0.4643, optimizer type was Rmsprop, learning rate was 0.0023, and batch size was 32. Conclusion: This method generates fault data through simulation to make up for the lack of samples, combines Bayesian optimization to improve the model's adaptability, enhances the accuracy of fault diagnosis, and provides technical support for the intelligent operation and maintenance of fire hydraulic systems.

Keywords

Fault Simulation; 1DCNN-Bayesian Optimization; Fault Diagnosis.

1. Introduction

With the acceleration of China's urbanization and industrialization, the pressure of fire prevention and control is increasing. The stability of the fire truck water pump system has become a core factor affecting the efficiency of fire fighting. However, fire pumps have long been affected by complex working conditions, environmental corrosion and mechanical aging, and the failure rate has increased significantly. Traditional diagnostic methods that rely on manual experience have limitations such as low efficiency, high misjudgment rate and scarce fault data, which are difficult to meet the real-time and accuracy requirements of modern fire protection systems.

In recent years, domestic and foreign scholars have conducted in-depth research on water pump system modeling and intelligent diagnosis technology, providing theoretical support for the construction of an efficient fault prediction system. In the field of system modeling, Gevorkov et al. [1]developed a centrifugal pump dynamic simulation model based on the Simulink platform, integrating centrifugal pumps, liquid storage tanks, regulating valves and other modules, and constructed a complete digital twin framework covering motor performance curves and pump characteristics analysis, laying the foundation for system behavior simulation and efficiency estimation. Kan K et al. [2]innovatively used the volume of fluid method (VOF) to simulate the dynamics of gas-liquid two-phase flow in response to the transient characteristics of power outages in pumping stations. Compared with the traditional rigid cover hypothesis (RLH) method, the prediction accuracy of the runaway speed was significantly improved, providing a key theoretical basis for the stability optimization of flood control and drainage systems. Kanchan Bharti et al. [3] studied and designed a solar automatic irrigation system, combined humidity sensing and MPPT maximum power tracking technology, and realized the intelligent start and stop of water pumps through an Arduino controller to reduce energy consumption and carbon emissions. However, the research still faces challenges such as insufficient field verification and lack of environmental adaptability assessment.

In the field of fault diagnosis, data-driven intelligent algorithms have shown significant advantages. The researchers extracted the time-frequency domain features of the vibration signal and combined it with a machine learning model to achieve fault classification. Saeid Farokhzad et al. [4] analyzed the vibration data of centrifugal pumps in healthy, impeller damaged, seal failure and cavitation states, extracted statistical features such as mean, skewness, and kurtosis, and constructed a single hidden layer neural network classifier. Experiments showed that its recognition accuracy for the four types of states reached 100%. Anil Kumar et al. [5] used genetic algorithm to optimize the parameters of support vector machine, which effectively improved the detection sensitivity of bearing defects; V. Muralidharan et al. [6] innovatively integrated wavelet transform, rough set and fuzzy logic to develop a multi-level decision model, which performed well in the coupled diagnosis of cavitation and mechanical faults. The introduction of deep learning technology has further promoted the breakthrough of diagnostic accuracy. Wasim Zaman et al. [7] generated vibration time-frequency spectrum through S transform, combined with Sobel edge detection and convolutional neural network (CNN), and realized the refined extraction of fault features; Zahoor Ahmad et al. [8] proposed the information ratio principal component analysis method (Ir-PCA), which improved the accuracy of K nearest neighbor classifier to 97.3% through multi-domain feature fusion and dimensionality reduction processing.

Aiming at the pain points of the lack of fault data of fire hydraulic system and the insufficient generalization ability of traditional methods, this paper proposes a hybrid diagnosis framework integrating physical simulation and deep learning. First, a simulation model of the fire hydraulic system is built based on Simscape to simulate typical fault conditions such as impeller wear, motor turn-to-turn short circuit, valve blockage, and pipeline leakage, and generate a simulation data set covering multi-dimensional features such as inlet and outlet pressure difference, vacuum, pipeline flow, and pump speed. Secondly, a simulation data set is used to compare the 1DCNN model with manual parameter adjustment and the 1DCNN model with the Bayesian optimization algorithm. The experiment shows that the 1DCNN driven by Bayesian optimization can effectively realize the fault diagnosis of the fire hydraulic system.

2. Algorithm Flow of 1DCNN-Bayesian Optimization Model

2.1 Basic Principles of 1DCNN

2.1.1 One-dimensional Convolution Operation

The core of 1DCNN is the one-dimensional convolutional layer[9], whose mathematical expression is:

$$y_i^{(l)} = \sum_{k=0}^{K-1} w_k^{(l)} \cdot x_{i+k}^{(l-1)} + b^{(l)} \tag{1}$$

In the formula, $x^{(l-1)}$is the input feature of the $l-1$th layer, with a dimension of $L \times C_{in}$ (L is the sequence length, C_{in} is the number of input channels); $w^{(l)}$is the convolution kernel weight of the

lth layer, with a size of $K \times C_{in} \times C_{out}$ (K is the convolution kernel length, C_{out} is the number of output channels); $b^{(l)}$ is the bias term; $y_i^{(l)}$ is the output value of the lth position of the ith layer. The convolution kernel slides along the input sequence, covering K consecutive points each time to generate local feature responses. Multi-channel convolution can extract features of different frequencies or shapes in parallel.

2.1.2 Non-linear Activation Function

To enhance the nonlinear expression ability of the model, the output of the convolutional layer needs to pass through the activation function:

$$z_i^{(l)} = \sigma\left(y_i^{(l)}\right) \tag{2}$$

Commonly used ReLU functions:

$$\sigma(y) = \max(0, y) \tag{3}$$

ReLU can alleviate the gradient vanishing problem and accelerate model convergence.

2.1.3 Pooling Layer

The pooling layer reduces the feature dimension and computational complexity by downsampling, while enhancing translation invariance. Pooling is divided into average pooling and maximum pooling. This study samples maximum pooling:

$$p_j^{l+1}(i) = max_{(i-1)w+1 \le t \le iw}\left\{a_j^l(t)\right\} \tag{4}$$

Where $a_j^l(t)$ represents the activation value of the tth neuron of the jth feature vector in the lth layer; w is the width of the pooling region; $p_j^{l+1}(i)$ is the pooling result corresponding to the neuron in the $l+1$th layer.

2.1.4 Fully Connected Layer and Classifier

The final feature map is flattened and input into the fully connected layer to output the fault category probability:

$$o = W_{fc} \cdot p + b_{fc} \tag{5}$$

$$P(c|x) = Softmax(o_c) = \frac{e^{o_c}}{\sum_{k=1}^{C} e^{o_k}} \tag{6}$$

Where C is the number of fault categories, W_{fc} and b_{fc} are the parameters of the fully connected layer.

2.2 The Principle of Bayesian Optimization

Using multi-sensor information as the analysis object requires a deeper network architecture to extract complex features. If the number of layers is too small, the network cannot extract sufficiently effective features, but too many layers in the network will lead to an explosive growth of hyperparameter combinations. Therefore, choosing the right hyperparameters has a great impact on network performance.

Bayesian optimization can find the next evaluation position based on the information obtained from the unknown objective function, so as to reach the optimal solution as quickly as possible[10]. In order to find a hyperparameter combination suitable for complex fault conditions of the fire hydraulic system and save tuning time, the Bayesian optimization algorithm is used to automatically select the optimal hyperparameter combination.

Bayesian optimization originates from Bayes' theorem, which uses the Bayesian formula to establish the probability distribution of the optimization process[11].

$$\begin{cases} p(g|D_{1:t} = \dfrac{p(D_{1:t}|g)p(g)}{p(D_{1:t})}) \\ D_{1:t} = \{(x_0, y_0), (x_1, y_1), \dots, (x_t, y_t)\} \end{cases} \tag{7}$$

In the formula, $g(\cdot)$ is the objective function used to evaluate performance; x_t is the decision vector; $y_t = g(x_t) + \varepsilon_t$ is the evaluation objective function value; ε_t is the observation noise; $D_{1:t}$ is the set of observed values; $p(D_{1:t}|g)$ is the likelihood distribution of the observed value y; $p(g)$ is the prior probability distribution of g, that is, the assumption about the state of the unknown objective function; $p(D_{1:t})$ represents the marginal likelihood distribution; $p(g|D_{1:t})$ is the posterior probability distribution of g, which describes the confidence of the unknown objective function after the prior is corrected by the observed data set.

The Bayesian optimization framework mainly consists of two core parts: the probabilistic proxy model and the acquisition function. This paper uses kernel density estimation (KDE) as a proxy model and probability improvement (PI) function as a collection function. First, the proxy model is used to fit the true target function; then the collection function is used to determine the next optimal sampling point from the unsampled area or the area where the optimal solution may appear based on the posterior probability of the past observation points; finally, the corresponding parameter set is updated until the stop condition is triggered. The parameter optimization process is expressed as:

$$\lambda_{t+1} = argmaxf(\lambda_t|D_{1:t}) \ \ (\lambda \epsilon \psi) \tag{8}$$

Where $f(\cdot)$ is the acquisition function; λ is the optimized parameter combination at time t; Ψ is the optimized parameter space.

2.3 1DCNN-Bayesian Optimization Model Fusion and Diagnosis Process

The 1DCNN-Bayesian optimization model is shown in 0 and is divided into two parts: the 1DCNN process and the Bayesian hyperparameter optimization process. In the 1DCNN process, the vacuum degree, inlet and outlet pressure difference, pump speed, and pipeline flow collected by the sensor are first used as network inputs; secondly, the fault features are extracted through the convolution layer; then the features are fused and passed to the Softmax output layer through the fully connected layer; finally, the probability value of each operating state is obtained, and the test accuracy is used as the output. The Bayesian optimization process will update the current hyperparameter combination based on the previous test accuracy and hyperparameter combination. The two processes are repeated until the termination condition is triggered.

This study uses kernel density estimation (KDE) as the proxy model and probability improvement (PI) function as the acquisition function to find the optimal solution hyperparameter combination. The specific steps are as follows.

(1) First, the acquisition parameters are obtained using the simulation system, and then the acquired parameters are preprocessed to establish a sample data set, which is divided into a training set and a validation set.

 Volume 11 Issue 5, 2025
DOI: 10.6919/ICJE.202505_11(5).0023

(2) Determine the network model and set the hyperparameters (network layers, convolution kernel size, number of convolution kernels, dropout parameter, optimizer, learning rate, batch-size) intervals to be optimized.

(3) Select a set of hyperparameters as the starting point to initialize the 1DCNN model, train the model and output the test accuracy.

(4) Perform Bayesian optimization, use kernel density estimation (GP) to represent the functional relationship of the hyperparameter combination on the 1DCNN model, and then select the next evaluation point through the probability improvement (PI) function, iteratively correct the prior information, and gradually improve the accuracy of the proxy model.

(5) After the Bayesian optimization is completed, return to the third step and reselect a set of hyperparameters for a new round of training until the number of iterations is reached.

(6) Output the set of hyperparameters and 1DCNN network model with the best model performance after Bayesian optimization.

(7) Input the test sample into the 1DCNN network model, and finally obtain the probability value of each operating state. The category with the highest probability is regarded as the final fault diagnosis result.

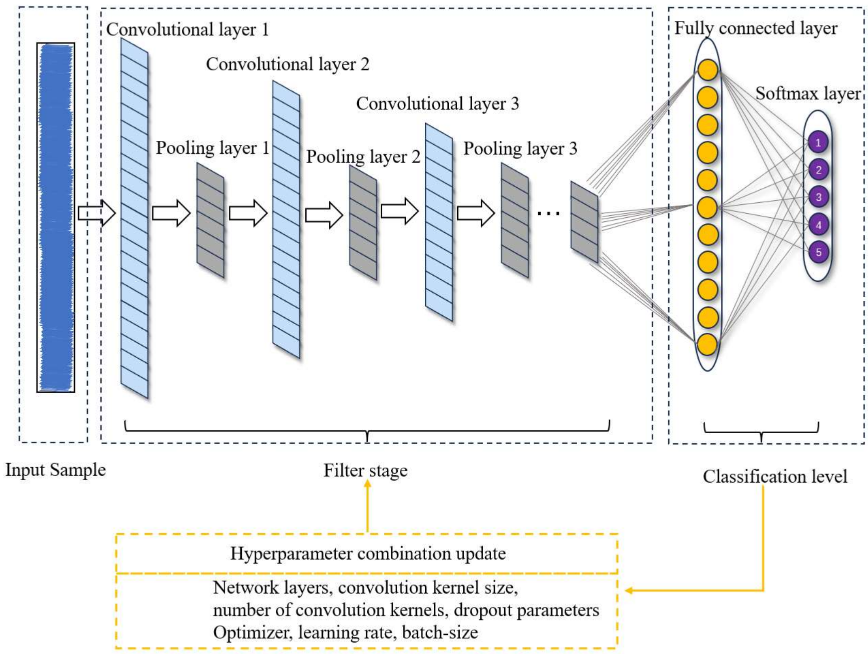

Figure 1. 1DCNN-Bayesian optimization fault diagnosis model

3. Fire Hydraulic System Fault Analysis and Simulation

The fire hydraulic system is mainly composed of four parts: induction motor, fire pump, valve and pipeline. When testing the system, the motor is connected to the pump shaft of the fire pump, and the pipeline is connected to the fire pump, valve and water tank to form a closed loop. The simulation system is shown in 0. The simulation of the motor turn-to-turn short circuit fault is shown in 0.

This study selected four faults corresponding to the four components, namely impeller wear, inter-turn short circuit, pipeline leakage and valve blockage, for simulation analysis. The fire pump uses Kaiquan XBD5/10-80 (W) horizontal single-stage fire pump and is configured according to its rated parameters; the Y2-160M1-2 model motor is selected, and the motor configuration is completed according to the rated parameters of this model. The rationality of the simulation data is verified according to the fitting degree of the rated performance curve of the water pump and the performance curve of the simulation data under normal working conditions. The fitting curve is shown in The

ISSN: 2414-1895
DOI: 10.6919/ICJE.202505_11(5).0023

simulation of the motor turn-to-turn short circuit fault is shown in 0. The root mean square error of the head-flow performance curve is 0.13m, and the error at Q=10L/s is 0.27%; the root mean square error of the effective shaft power-flow performance curve is 13.05w, and the error at Q=10L/s is 0.00%. This shows that the simulation model is reliable and the simulation data can support subsequent fault diagnosis.

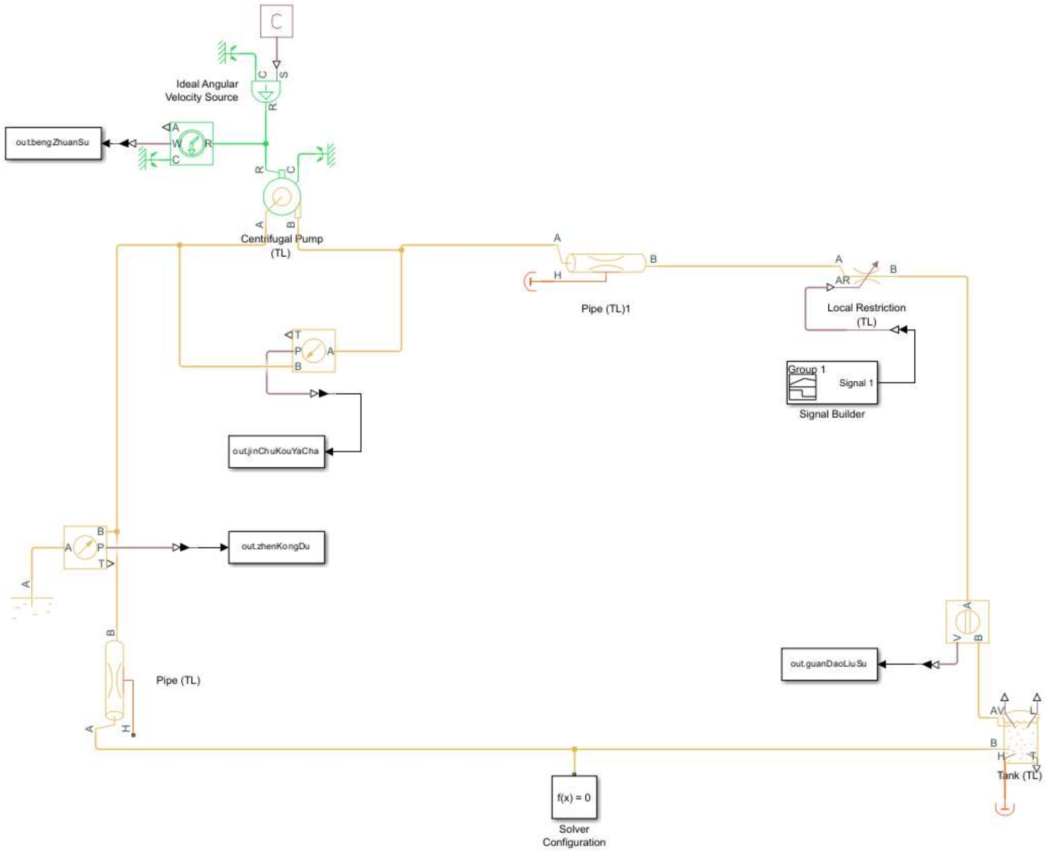

Figure 2. Fire Hydraulic System Simulation Model

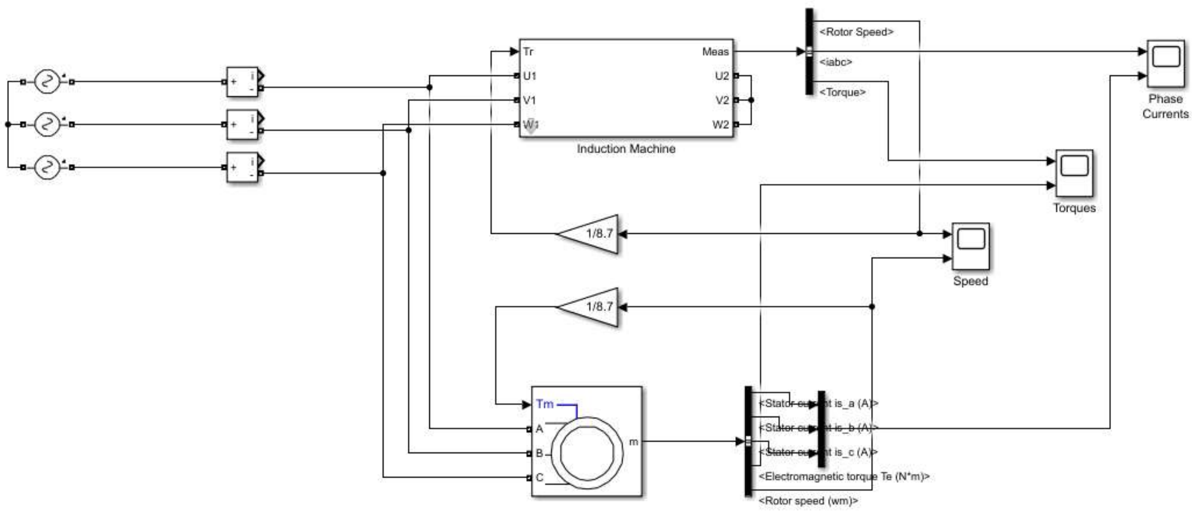

Figure 3. Fire Hydraulic System Simulation Model

ISSN: 2414-1895 DOI: 10.6919/ICJE.202505_11(5).0023

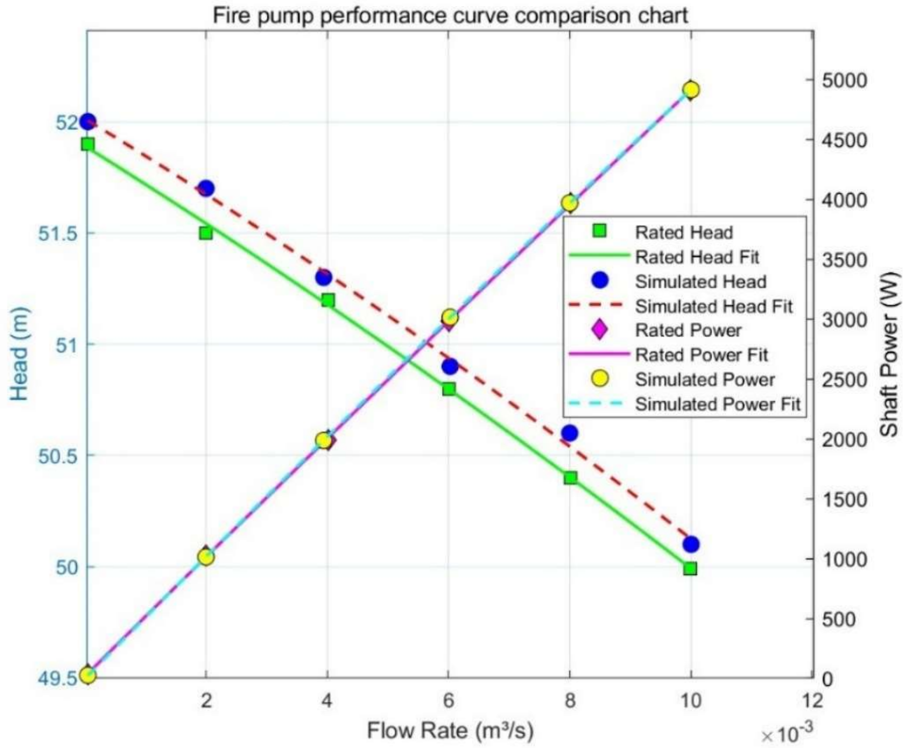

Figure 4. Fire pump performance curve comparison chart

4. Fire Hydraulic System Fault Diagnosis Experiment

4.1 Data Collection and Processing

Through the analysis of four types of faults in the fire pump impeller wear, pipeline leakage, valve blockage, and motor stator inter-turn short circuit in the fire hydraulic system, different fault injections are carried out on the built fire hydraulic system according to the nature of the fault, and the vacuum degree, inlet and outlet pressure difference, pump speed, and pipeline flow are used as outputs. Then, the information of the fire hydraulic system under normal state and four fault states is obtained by simulation.

For the faults of impeller wear, pipeline leakage, and valve blockage, the simulation system is connected to the ideal angular velocity source, and the simulation is performed for 100s when the valve opening is 100%, 80%, 60%, 40%, and 20%, and three different fault degrees are simulated respectively. The specific fault degrees are shown in 0. The proportional coefficient k_{wear} is set for impeller $\mathrm{k}_{wear}=0.3,0.5,0.7$; the pipeline leakage area is set to $0.0002m^2$, $0.0006m^2$, and $0.001m^2$ respectively; the valve blockage degree is determined by the valve opening area, which is set to $0.00005m^2$, $0.0001m^2$, and $0.00015m^2$ respectively. During simulation, the solver selected is ode15s, the maximum step size $\Delta t=1s$, the simulation time is once every 100 seconds, and the number of sampling points is 100×5×3=1500.

Table 1. Fault severity coefficient setting

Fault type	Fault parameters	Failure coefficient
Impeller wear	Wear ratio	0.3,0.5,0.7
pipeline leakage	Leakage area	$0.0002m^2$,$0.0006m^2$,$0.001m^2$
valve blockage	Effective area	$0.00005m^2$,$0.0001m^2$,$0.00015m^2$
turn-to-turn short circuit	Failure coefficient	0.1,0.2,0.3,0.4,0.5,0.6,0.7,0.8,0.9,0.95

For the short-circuit fault between stator turns of the motor, the simulation system is connected to the faulty motor, and the motor reaches the steady state from the starting state in about 10s. The fault coefficient is set to 0.1, 0.2, 0.3, 0.4, 0.5, 0.6, 0.7, 0.8, 0.9, and 0.95, and the simulation is performed for 40s respectively. In the simulation process of the last 30s, the step signal of the valve opening of 100%, 50%, and 25% is configured for 10s each. During the simulation, the solver is selected as ode15s, the maximum step length $\Delta t = 1 \times 10^{-4} s$, each simulation time is 40 seconds, and the number of sampling points is about 800000. Due to the short sampling step length of the stator turn short circuit fault and the dense number of sampling points, in order to include more periodic signals within the limited time series length, the output signal is downsampled, corresponding to the general sampling frequency of 1s in industry, and the number of samples collected in the simulation of 40s is reduced to 40. The number of sampling points obtained in the end is $40 \times 10 = 400$.

Then divide the data into time series segments of fixed length, and set the sample length l = 10 to construct a standardized time series sample set. Then use the minimum-maximum normalization for each signal x to scale the data of each time series segment to the interval [0, 1]. The minimum-maximum normalization is shown in Equation 9.

$$x' = \frac{x - x_{min}}{x_{max} - x_{min}} \tag{9}$$

In addition, this paper proposes an overlapping sampling enhancement method based on sliding windows. As shown in Formula 10, the original continuous signal is dynamically segmented with a preset overlapping rate λ, and subsequence samples with time series correlation are generated by window sliding, and the training set, validation set and test set are constructed accordingly.

$$\begin{cases} m = floor(\frac{L - l}{l\lambda}) \\ x_i' = x'[((i-1) \times l \times (1-\lambda)):((i-1) \times l \times (1-\lambda) + l)] \end{cases} \tag{10}$$

In the formula, m is the maximum number of split samples per signal; $floor(\cdot)$ is the rounding function; L is the length of each signal; l is the sample length set; λ is the overlap rate; x_i' is the ith data sample after segmentation, $i \in [i, m]$; x' is the normalized signal.

This study initially sets the sample length $l = 10$, and splits the $l = 10$ signal with an overlap rate λ of 1/3 to achieve sample set expansion. 80% of these samples are designated as training sets, 10% as validation sets, and 10% as test sets. Specific sample information is shown in 0.

Table 2. Experimental sample information

Fault state	Fault Tags	Total number of samples
Normal state	0	2500
Valve blockage	1	1500
Pipeline leakage	2	1500
Impeller wear	3	1500
Motor turn short circuit	4	400

4.2 Hyperparameter Selection

This study selected the 1DCNN model after manual parameter adjustment and the 1DCNN model after Bayesian optimization for comparative experiments. In the Bayesian optimization algorithm,

ISSN: 2414-1895 DOI: 10.6919/ICJE.202505_11(5).0023

seven hyperparameters (network layers, convolution kernel size, number of convolution kernels, dropout parameter, optimizer type, learning rate, batch size) are selected to set the optimization interval. The optimization interval is determined by experiments and experience. The specific optimization interval is shown in 0.

Table 3. Hyperparameter Ranges

Hyperparameters	Parameter range
Number of network layers	[2,4]
Convolution kernel size	[3,5,7,11,15,20]
Number of convolution kernels	[32,64,128,256]
Dropout parameter p	[0.3,0.6]
Optimizer type	[SGD, Adadelta, Adam, RMSprop]
Learning rate	[0.0001,0.01]
Batch-size	[16,32,64,128]

After continuous iterative optimization of the 1DCNN model hyperparameter combination using the Bayesian optimization algorithm and continuous training of the model under different parameter combinations, the optimal parameter combination is obtained. The hyperparameter values of the original manually adjusted 1DCNN and 1DCNN-Bayesian models are shown in Table 4.

Table 4. Hyperparameter settings of original 1DCNN and 1DCNN-Bayesian optimization

Hyperparameters	Original 1DCNN value	1DCNN-Bayesian optimization value
Number of network layers	3	3
Convolution kernel size 1	20	20
Number of convolution kernels 1	32	32
Convolution kernel size 2	20	5
Number of convolution kernels 2	64	64
Convolution kernel size 3	20	3
Number of convolution kernels 3	128	128
Dropout parameter p	0.5	0.4643
Optimizer type	RMSprop	RMSprop
Learning rate	0.001	0.0023
Batch-size	32	32

4.3 Experiment and Result Analysis

The 1DCNN model was constructed according to the optimal hyperparameters obtained in Section 3.2, and the processed simulation data was passed into the network for testing. The training cycle (Epochs) was set to 100. The loss value curve and accuracy curve of the training process are shown in The simulation of the motor turn-to-turn short circuit fault is shown in 0. When the number of iterations is about 30, the accuracy curve tends to be stable and fluctuates within a small range. At the end of the training, the final fault diagnosis rate reaches 98.1%.

Volume 11 Issue 5, 2025
DOI: 10.6919/ICJE.202505_11(5).0023

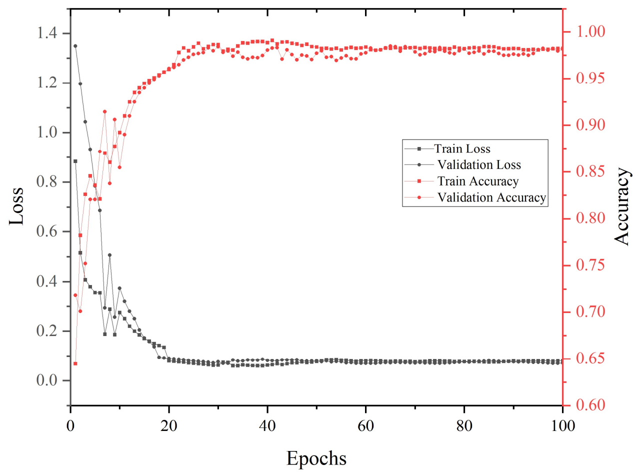

Figure 5. 1DCNN-Bayesian optimization fault diagnosis training results

In order to more intuitively show the diagnosis results of the model for fire hydraulic system faults, the confusion matrix of the best result shown in The simulation of the motor turn-to-turn short circuit fault is shown in 0. is used for illustration. The horizontal axis in The simulation of the motor turn-to-turn short circuit fault is shown in 0.represents the expected output label, and the vertical axis represents the true output label. The values on the diagonal represent the correct classification results of each category by the network model in this paper. The values in other positions outside the diagonal represent the misclassification results of each category. It can be observed that the 1DCNN-Bayesian optimization algorithm proposed in this chapter shows a high accuracy in the fault diagnosis of fire hydraulic system. For five different states (normal, valve blockage, pipeline leakage, impeller wear, motor inter-turn short circuit), except for one sample in the normal state (label 0) that was misjudged as an electronic inter-turn short circuit, the diagnostic accuracy of the other four state types reached 100%. This shows that the algorithm has a high recognition ability for various fault types of fire hydraulic system.

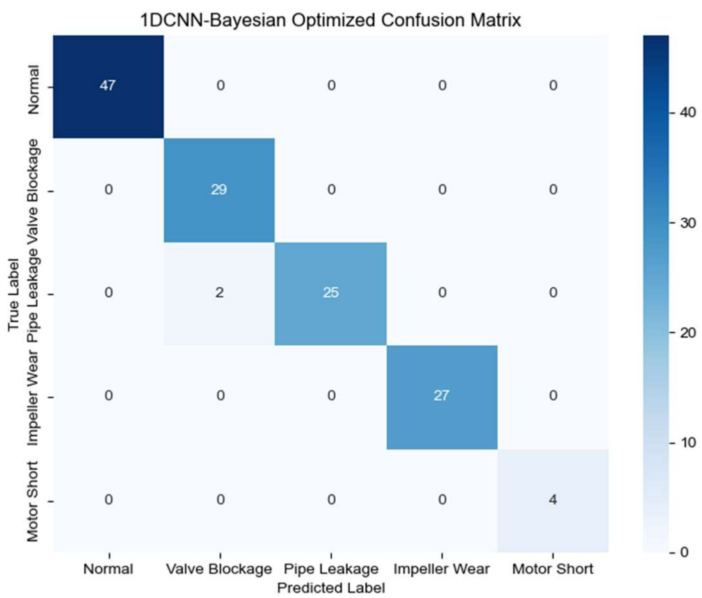

Figure 6. 1DCNN-Bayesian Optimized Confusion Matrix

ISSN: 2414-1895 DOI: 10.6919/ICJE.202505_11(5).0023

0 compares the training effects of 1DCNN and 1DCNN-Bayesian models. It can be seen from the table that the training effect of 1DCNN after Bayesian optimization is better than that of the original 1DCNN. The accuracy of 1DCNN-Bayesian model is 98.51%, and the accuracy of 1DCNN is 97.01%. The accuracy of 1DCNN-Bayesian is higher than that of 1DCNN model.

Table 5. Performance comparison between the original 1DCNN and 1DCNN-Bayesian models

Classification Model	Macro-Precision (%)	Macro-Recall(%)	F1(%)
1DCNN	97.58	97.04	97.11
1DCNN-Bayesian	98.71	98.52	98.56

5. Conclusion

In view of the fact that the traditional fire hydraulic system fault diagnosis method is too much combined with the actual operation experience of relevant staff, it is difficult to ensure the timeliness and accuracy of fault diagnosis, as well as the problems of multiple monitoring signals, easy signal distortion, and difficulty in obtaining fault data in the actual production of fire hydraulic systems, this paper proposes a fire hydraulic system fault diagnosis method that integrates simulation modeling and 1DCNN-Bayesian optimization algorithm, and verifies its effectiveness through experiments. The main conclusions are as follows:

(1) Simscape is used to build a fire hydraulic system simulation platform. The system covers four core components: fire pump (simulating impeller wear fault), motor (simulating stator inter-turn short circuit fault), valve (simulating blockage fault) and pipeline (simulating leakage fault). Through mechanism modeling and parameterized fault injection, a simulation data set containing multi-dimensional sensor data such as speed, inlet and outlet pressure, vacuum degree and flow rate is generated. The performance curves of the simulation data and the rated operating condition data are compared (for example, the root mean square error of the head-flow performance curve is 0.13m, and the error at Q=10L/s is 0.27%; the root mean square error of the shaft effective power-flow performance curve is 13.05w, and the error at Q=10L/s is 0.00%), which verifies the physical rationality and data transferability of the simulation model.

(2) In order to further improve the diagnostic robustness, the Bayesian optimization algorithm is introduced to automatically adjust the parameters. The kernel density estimation (KDE) is used as the surrogate model, and the probability improvement (PI) function is used as the acquisition function to model the hyperparameter space. After 50 rounds of iterations, the optimal configuration is obtained: three-layer convolution (kernel size [20, 5, 3], number of filters [32, 64, 128]), Dropout parameter is 0.4643, optimizer type is Rmsprop, learning rate is 0.0023, and batch size is 32. The accuracy of the optimized model reached 98.51%, which is 1.50% higher than the accuracy of the original 1DCNN model.

References

[1] Gevorkov L, Rassõlkin A, Kallaste A, et al. Simulink based model for flow control of a centrifugal pumping system[C]. 2018 25th International Workshop on Electric Drives: Optimization in Control of Electric Drives (IWED). IEEE, 2018: 1-4.

[2] Kan K, Chen H, Zheng Y, et al. Transient characteristics during power-off process in a shaft extension tubular pump by using a suitable numerical model[J]. Renewable Energy, 2021, 164: 109-121.

[3] Bharti K, Singh S K, Jha S K, et al. Modelling and simulation of solar water pump using arduino uno in Proteus[C]//2023 International Conference on Intelligent and Innovative Technologies in Computing, Electrical and Electronics (IITCEE). IEEE, 2023: 774-781.

[4] Farokhzad S, Ahmadi H, Jaefari A, et al.Artificial neural network based classification of faults in centrifugal water pump[J].Journal of Vibroengineering.2012, 14(4).

ISSN: 2414-1895
DOI: 10.6919/ICJE.202505_11(5).0023

[5] Kumar A, Kumar R.Time-frequency analysis and support vector machine in automatic detection of defect from vibration signal of centrifugal pump[J].Measurement.2017, 108: 119-133.

[6] Muralidharan V, Sugumaran V.Rough set based rule learning and fuzzy classification of wavelet features for fault diagnosis of monoblock centrifugal pump[J].Measurement.2013, 46(9): 3057-3063.

[7] Zaman W, Ahmad Z, Siddique M F, et al. Centrifugal Pump Fault Diagnosis Based on a Novel SobelEdge Scalogram and CNN[J]. Sensors, 2023, 23(11): 5255.

[8] Ahmad Z, Nguyen T K, Ahmad S, et al. Multistage centrifugal pump fault diagnosis using informative ratio principal component analysis[J]. Sensors, 2021, 22(1): 179.

[9] Wu J. Introduction to convolutional neural networks[J]. National Key Lab for Novel Software Technology. Nanjing University. China, 2017, 5(23): 495.

[10] Frazier P I. Bayesian optimization[M]//Recent advances in optimization and modeling of contemporary problems. Informs, 2018: 255-278.

[11] Joyce J. Bayes' theorem[J]. 2003.